Supplementary Material

Carbon Dots on Laponite Hybrid Nanocomposites: Solid-state emission and Inter-aggregate Energy Transfer

Bruno S. D. Onishi,[1,2] Albano N. Carneiro Neto,[1] Ricardo Bortolleto-Santos,[3] Valmor R. Masterlaro,[4] Luís D. Carlos,[1] Rute A. S. Ferreira,[1,*] Sidney J. L. Ribeiro[2,*]

[1] Department of Physics and CICECO – Aveiro Institute of Materials, University of Aveiro, 3810-193 Aveiro, Portugal

[2] Institute of Chemistry, São Paulo State University─UNESP, São Paulo, Araraquara, 14800-060, Brazil

[3] Postgraduate Program in Environmental Technology, University of Ribeirão Preto─UNAERP, São Paulo, Ribeirão Preto, 14096-900, Brazil

[4] São Carlos Institute of Chemistry, University of São Paulo─USP, São Paulo, São Carlos, 13566-590, Brazil.

* Corresponding authors: rferreira@ua.pt (Rute A. S. Ferreira); sidney.jl.ribeiro@unesp.br (Sidney J. L. Ribeiro)

Contents

Supplementary Material

Supplementary Material

Table S1 - Data of angle 2θ diffracted planes and interlayer distance (d) calculated by Bragg's Law.

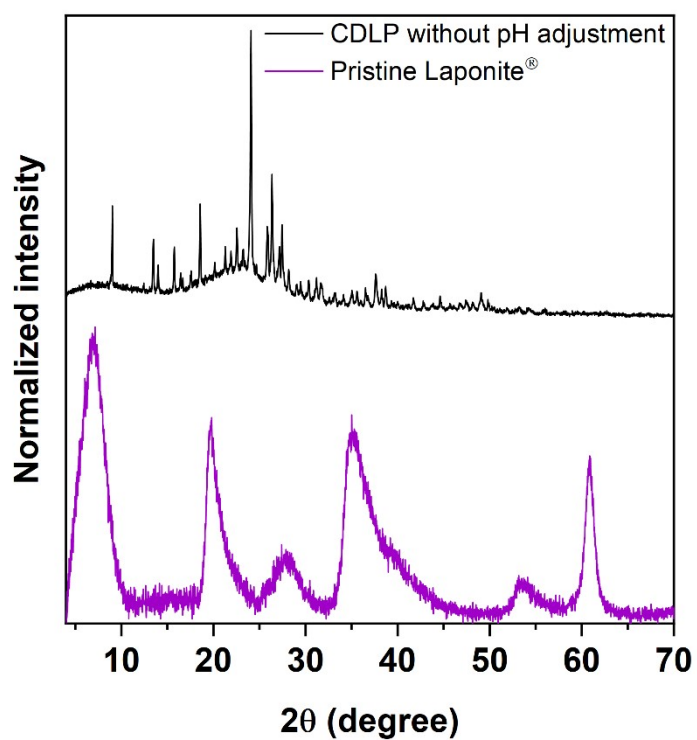| Samples	2θ (degree)	d (Å)
CDLP-A	6.75	13.08 ± 0.08
CDLP-B	6.70	13.18 ± 0.08
CDLP-C	6.70	13.18 ± 0.08
CDLP-D	6.67	13.18 ± 0.08
Lap	6.96	12.69 ± 0.07
Pristine Laponite	6.92	12.76 ± 0.07

Figure S1. Powder X-Ray Diffraction (PXRD) patterns of CDLP without pH adjustment (pH = 5) and pristine Laponite.
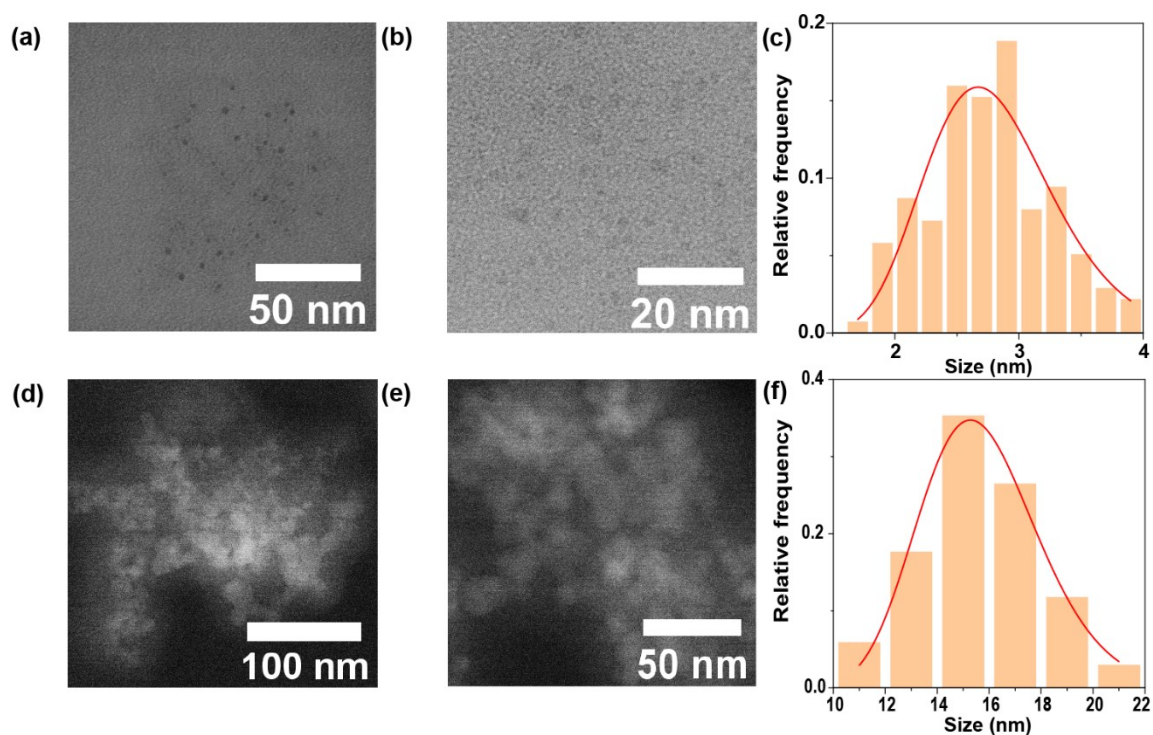
Supplementary Material

Figure S2. Scanning Transmission Electron Microscopy (STEM) (a) images of CDLP-D (b) with size distribution in (c); STEM images of CD (d) and (e) with size distribution in (f). The histogram of nanoparticle's size distribution was generated by counting at least 150 nanoparticles from several images obtained. The red solid line represents the fitted log-normal distribution, providing an average particle size of 2.8 $\pm$ 0.5 nm for CDLP-D and 15.8 $\pm$ 2.3 nm.
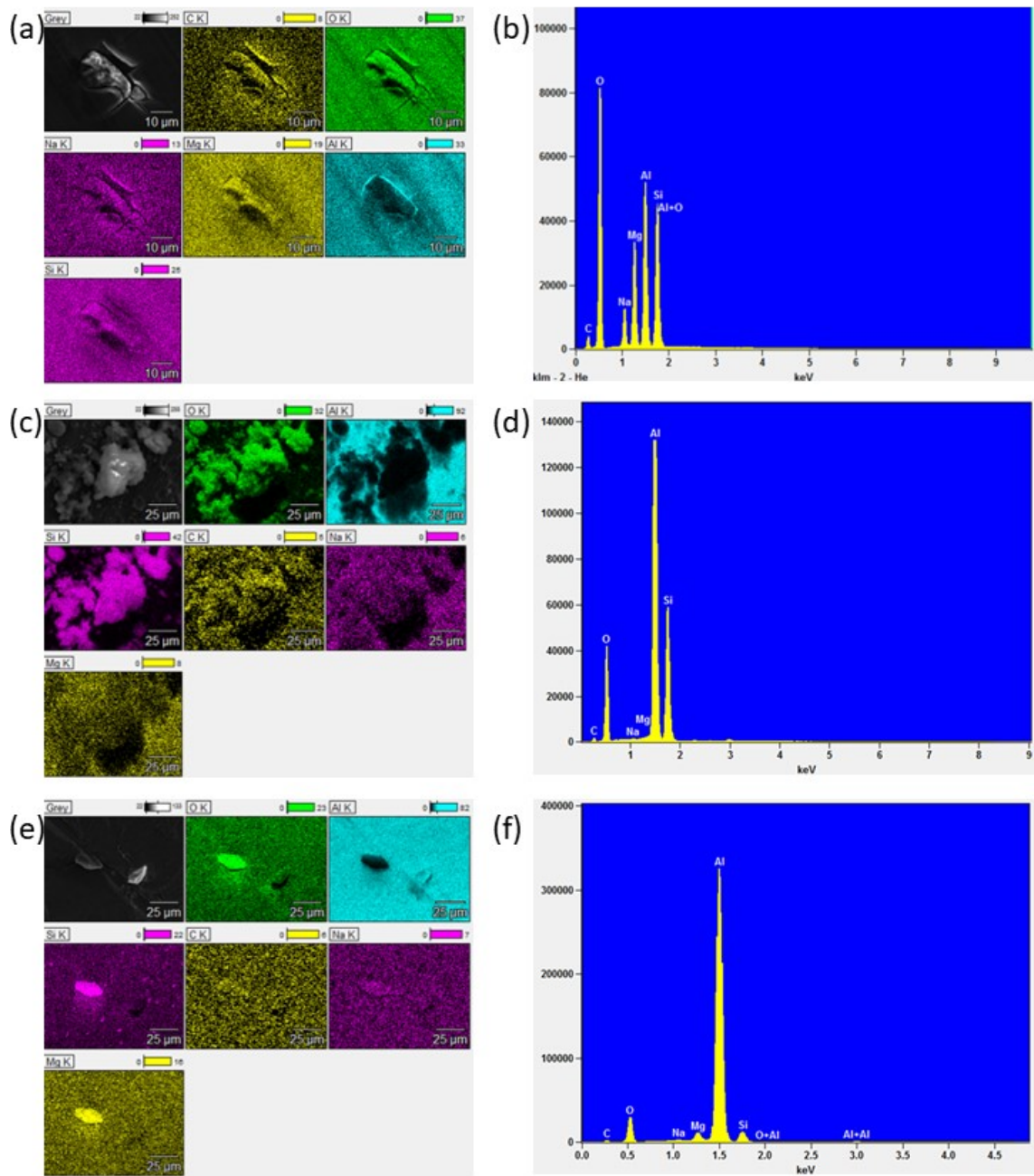
Figure S3. EDX mapping using SEM microscope coupled with EDX spectrometer for CDLP-A (a), CDLP-D (c) and Lap (e); with the respective EDX spectrum (b), (d) and (f). The alluminum content is from the substrate used.

Supplementary Material

Table S2 - FTIR band assignments for the bonds vibrations of the samples in the region of 4000 - 410 cm-1; ν represents stretching, and δ deformation

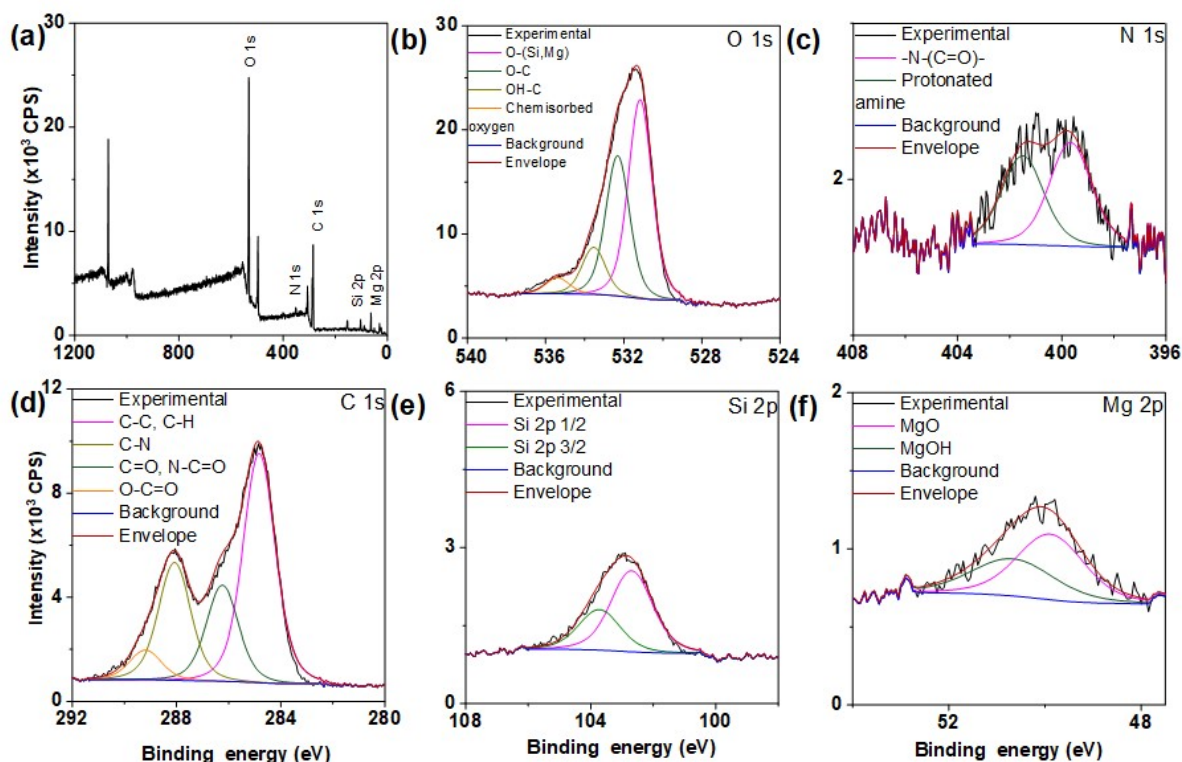| Wavenumber (cm^{-1})	Assignment	Refs
3690	ν(Mg$_3$OH)	[37]
3720 – 3000	ν(OH)/ ν(NH)	[38,39]
2934	ν(CH)	[38,39]
1774	ν(C=O) – conjugation with oxygen	[38,39]
1704	ν(C=O) – amide	[38,39]
1656	δ(NH)	[38,39]
1632	δ(OH) – adsorbed water	[38,39]
1596	ν(COO) – carboxylate asymmetric	[40–42]
1552	ν(C=C)/ ν(C=N) – aromatic ring	[38,39]
1440	δ(CH)	[38,39]
1392	ν(COO) – carboxylate symmetric/ δ(C–N)	[40–42]
1296	δ(COH)	[38,39]
1172	ν(CO)	[38,39]
966	ν(SiO)	[37]
643	δ(MgO)	[37]
430	δ(Si–O–Si)	[37]

Figure S4. X-Ray Photoelectron Spectroscopy survey spectrum of CDLP-D (a); high-resolution XPS spectrum of O 1s (b), N 1s (c), C 1s (d), Si 2p (e) and Mg 2p (f) of CDLP-D sample.
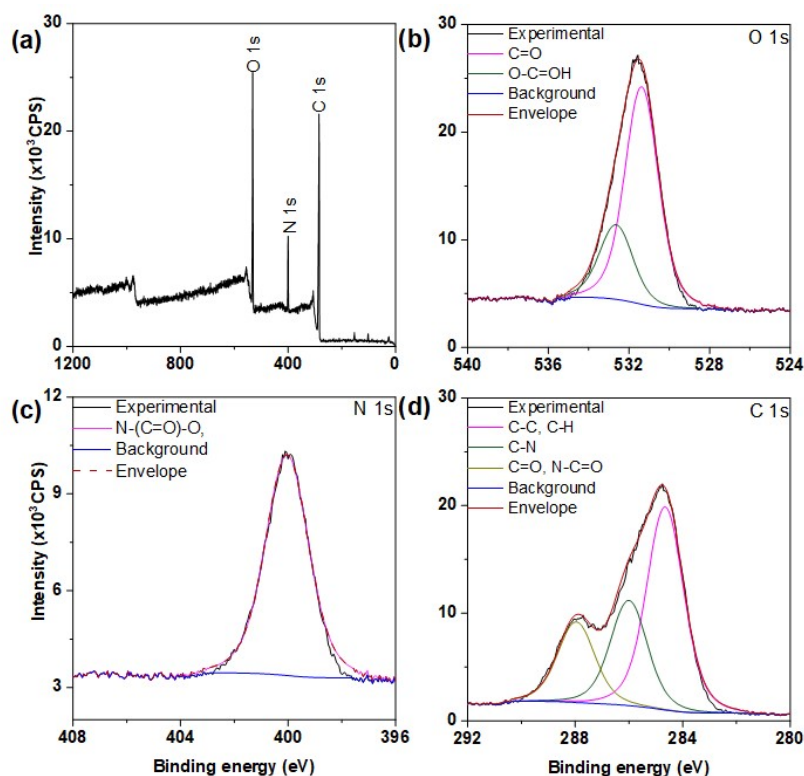

Figure S5. XPS survey spectrum of CD (a); high-resolution XPS spectrum of O 1s (b), N 1s (c) and C 1s (d) of CD sample.
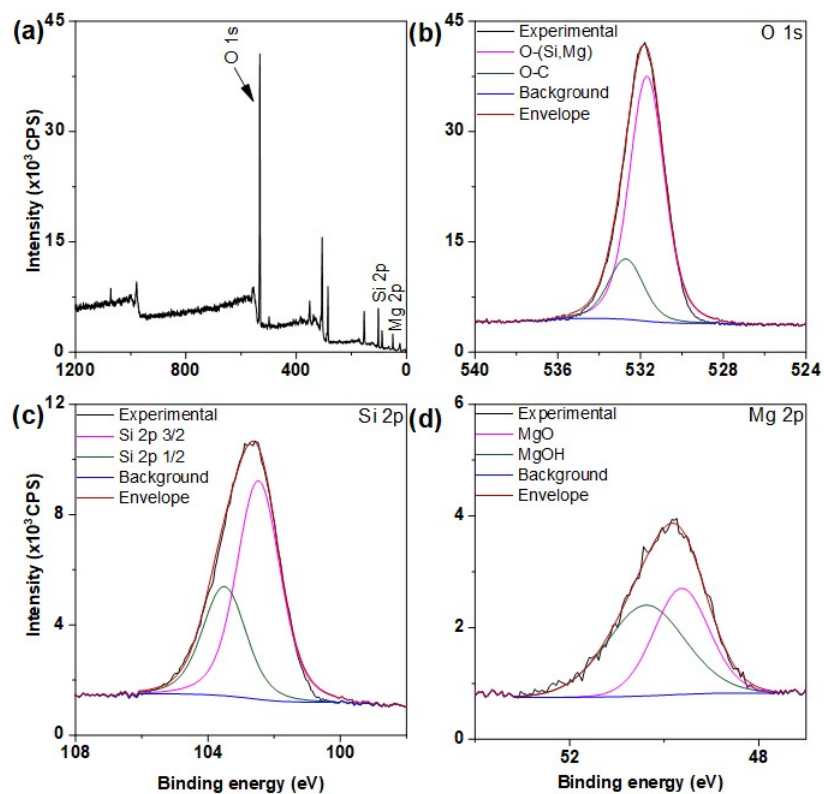
Supplementary Material

Figure S6. XPS survey spectrum of Lap (a); high-resolution XPS spectrum of O 1s (b), Si 2p (c) and Mg 2p (d) of Lap sample.
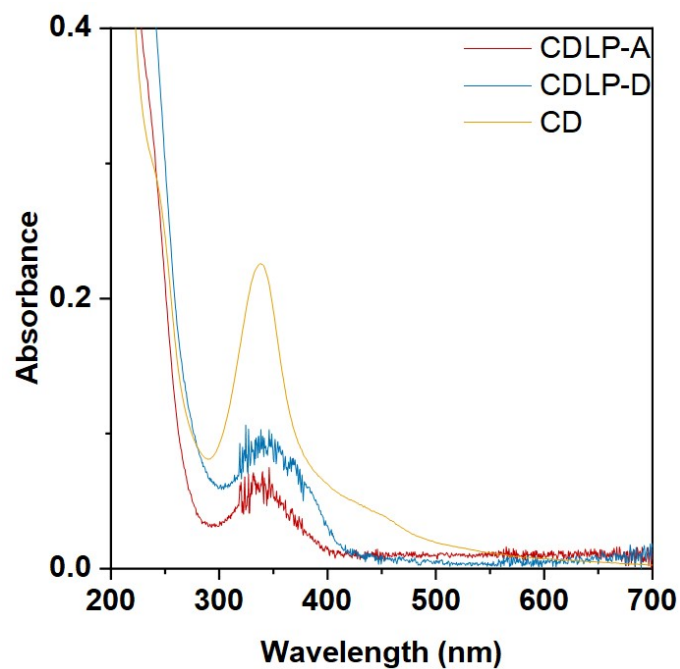

Figure S7. UV-Vis spectrum in the 200 – 800 nm range of 1.0 mg·mL^{-1} water suspension of CD, CDLP-A, and CDLP-D samples.
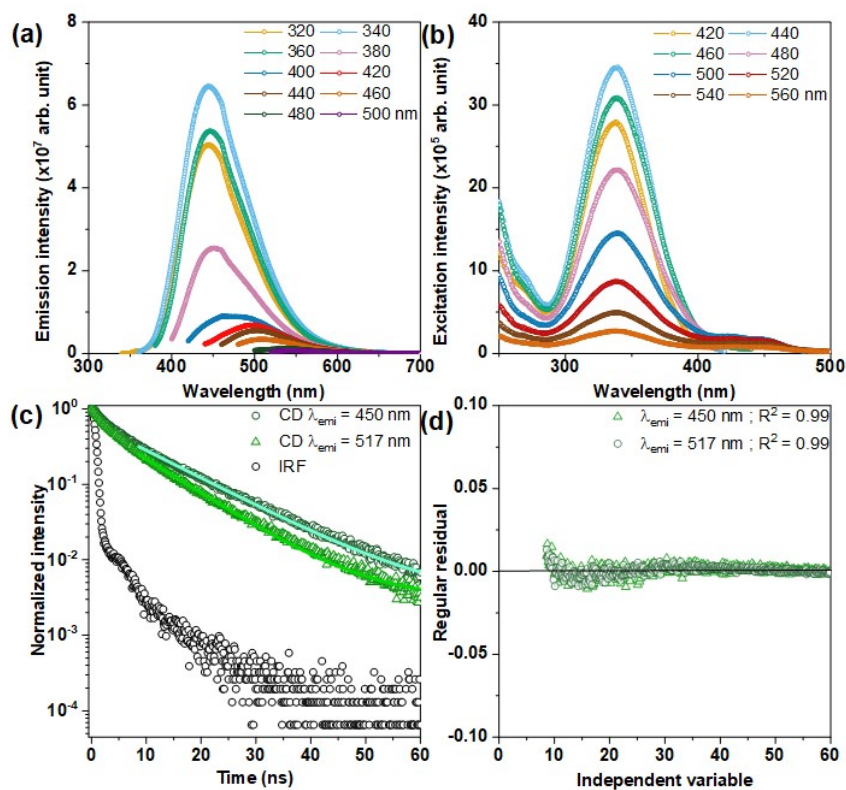
Supplementary Material

Figure S8. Room temperature (298 K) (a) emission and (b) excitation spectra of CD in water suspension. (c) Room temperature emission decay of CD suspension using a 388 nm nano-LED monitoring emission at 450 and 517 nm. (d) Residual plots of the monoexponential fitting on the decay curves presented in (c). For suspension, the quantum yield (ϕ) at excitation wavelengths of 360, 400, and 500 was 0.06 ± 0.01, 0.03 ± 0.01 and 0.01 ± 0.01 respectively; for solid sample in all excitation wavelengths, the ϕ was below 0.01. The lifetime obtained by monoexponential fitting in the emission decay curve for suspension was 12.0 ± 1.2 and 9.4 ± 0.9 ns for 450 and 517 nm wavelength emission, respectively.
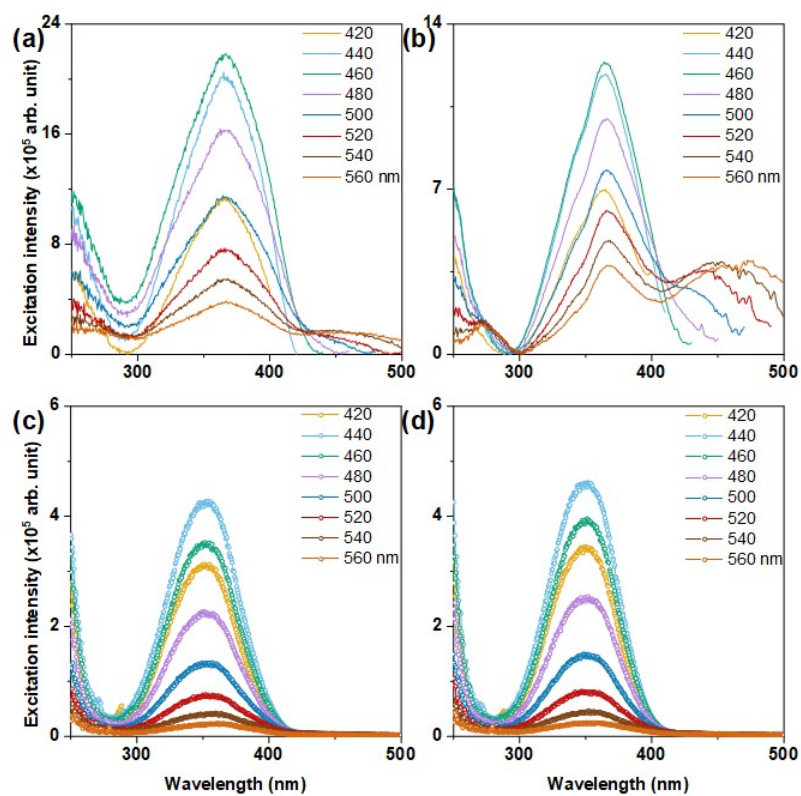
Supplementary Material

Figure S9. Room temperature excitation spectra of CDLP-A in (a) powder and (c) water suspension and CDLP-D in (b) powder and (d) water suspension, respectively.
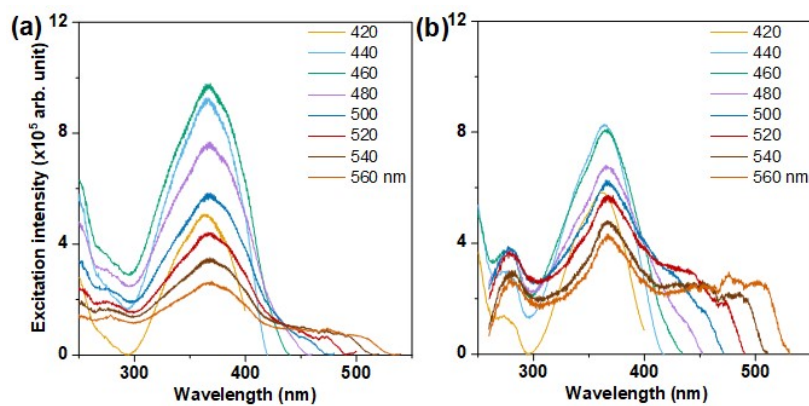

Figure S10. Low temperature (13 K) excitation spectrum of (a) CDLP-A and (b) CDLP-D.
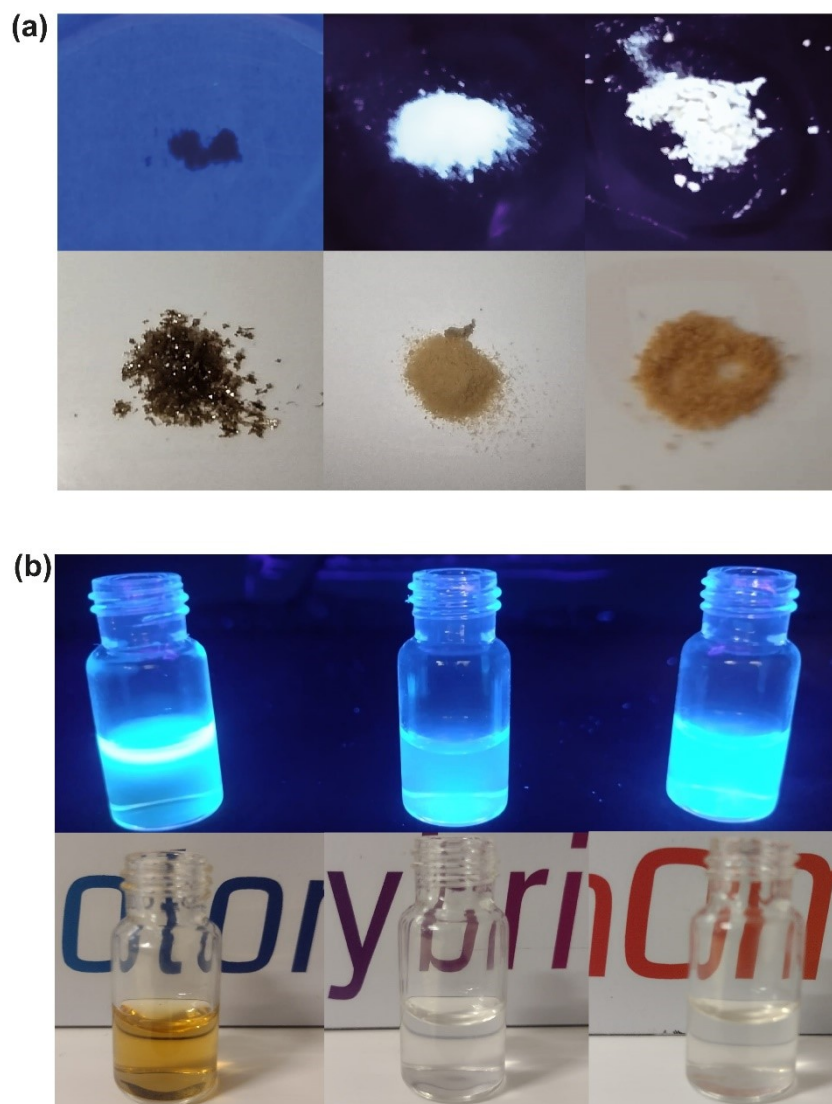
Supplementary Material

Figure S11. Photographs of powder (a) and water suspension (b) samples, with UV lamp ($\lambda_{exc} = $ 365 nm) above and room light below. From left to right: CD, CDLP-A and CDLP-D.
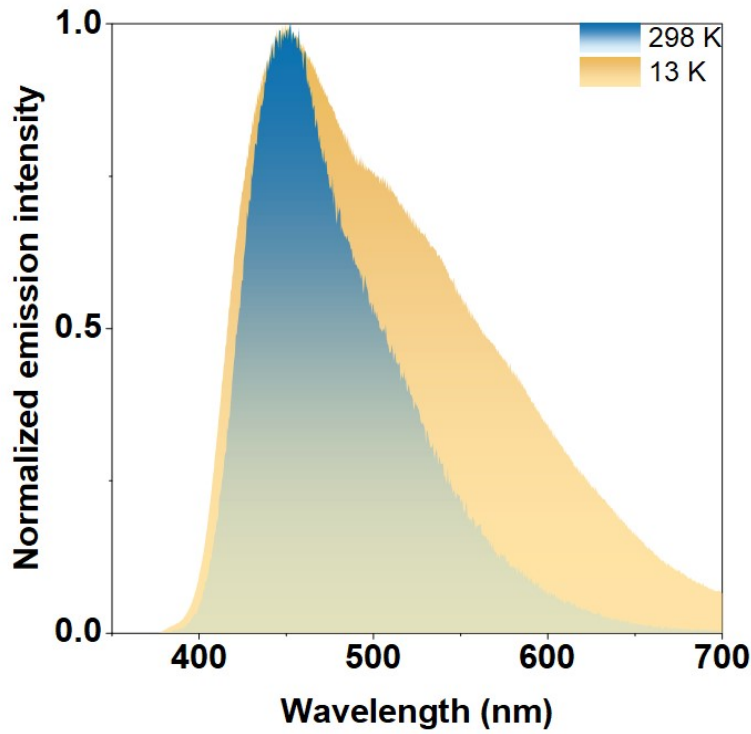
Supplementary Material

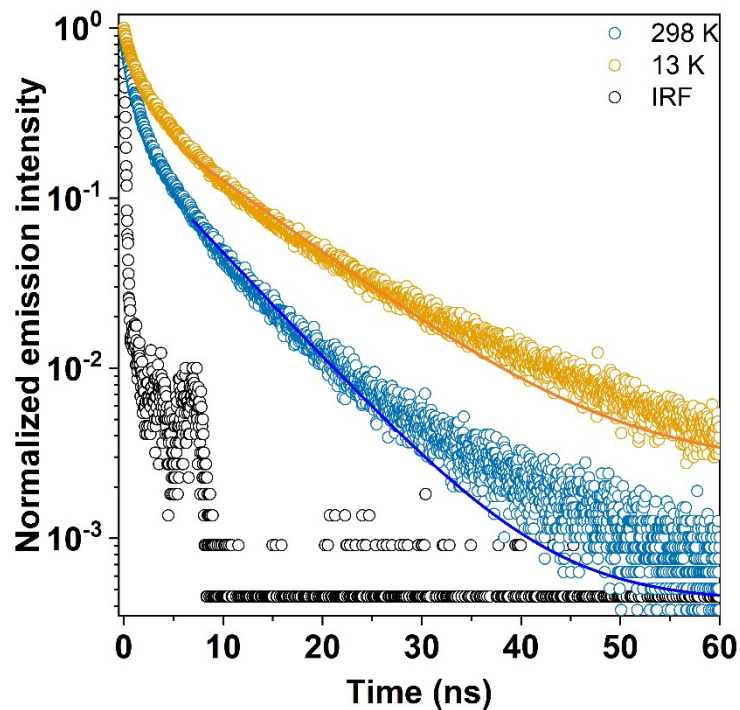**Figure S12.** Room and low temperature emission comparison of CDLP-A.

Figure S13. Room and low temperature decay curves of CDLP-D monitored at 450 nm and excited at 375 nm using a nano-LED. IRF is the instrumental response function. The model used was

$$y = y_0 + \sum_n A_n exp\boxed{}(-(t_n - x_0)/\tau_n)$$

, where y is the PL intensity, y_0 is a constant, A_n the amplitude of the n component of the decay, t_n is the experimental decay data, and $x_0 = 6.96$ ns is obtained by the instrument response function. The best fitting was achieved by applying

one component. Lifetime obtained at 298 K was $\tau_{450}^{298} = 7.0 \pm 0.1$ ns and at 13 K was $\tau_{450}^{13} = 10.0 \pm 0.1$ ns.
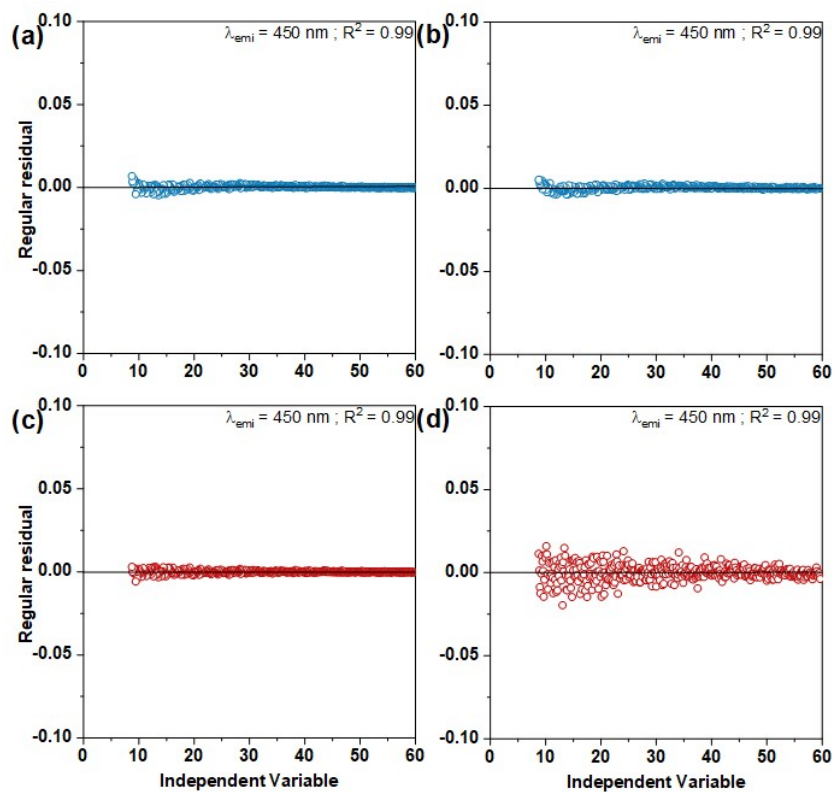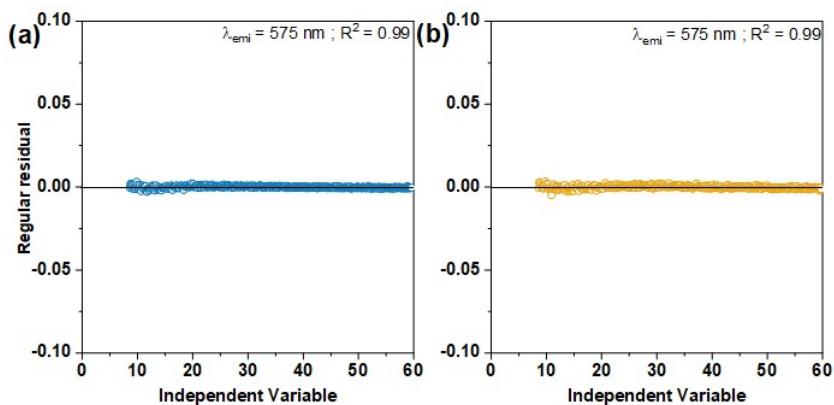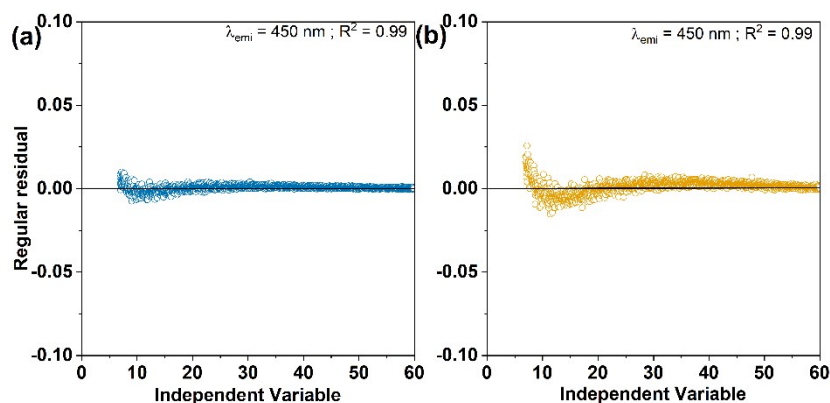

Figure S14. Residual plots of the monoexponential fits of the room temperature emission decay curves at 450 nm of CDLP-A (a) powder and (c) suspension and CDLP-D (b) powder and (d) suspension. A 388 nm nano-LED was used as the excitation source.
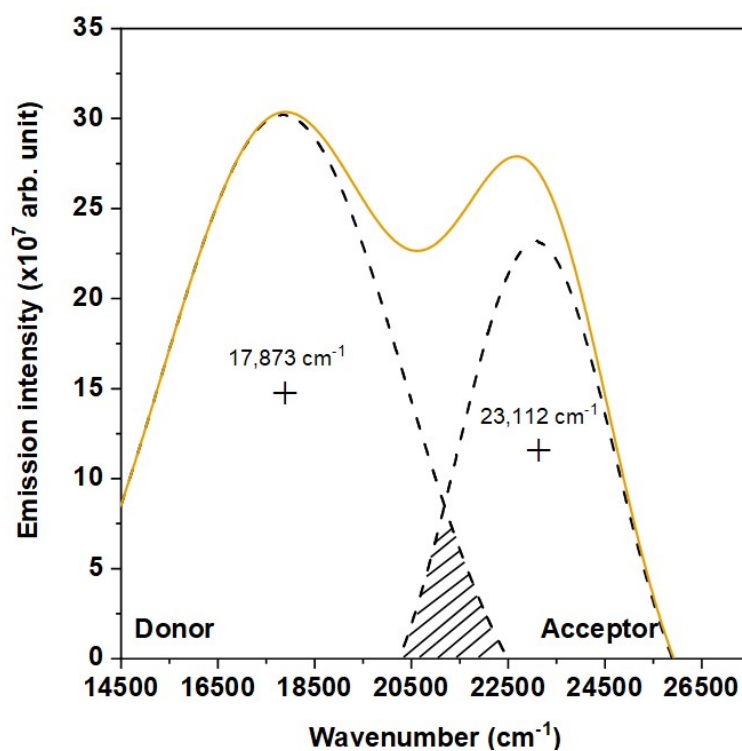
Supplementary Material

Figure S15. Residual plots of the monoexponential fits of the (a) room and (b) low temperature emission decay curves at 575 nm of CDLP-D. A 388 nm nano-LED was used as the excitation

source.

Figure S16. Residual plots of the monoexponential fits of the (a) room and (b) low temperature emission decay curves at 450 nm of CDLP-D. A 375 nm nano-LED was used as the excitation source.

Figure S17. Deconvolution of CDLP-D emission band with respective barycenter. $\sigma_D = 17{,}873$ cm^{-1} with $\gamma_D = 5{,}194$ cm^{-1} and $\sigma_A = 23{,}112$ cm^{-1} with $\gamma_A = 3{,}232$ cm^{-1}.
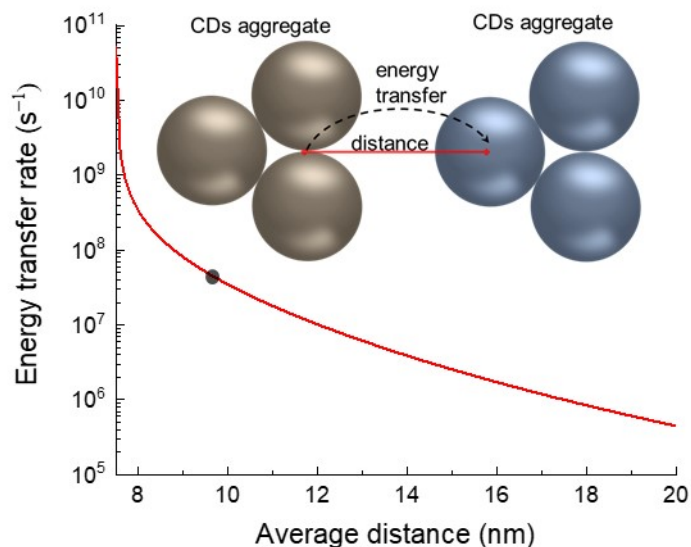

Figure S18. Estimated energy transfer rate between CDs aggregates as a function of their average distance. The black point corresponds to the experimental rate $W = 4.7 \times 10^7$ s^{-1} attributed to the distance of 9.6 nm.
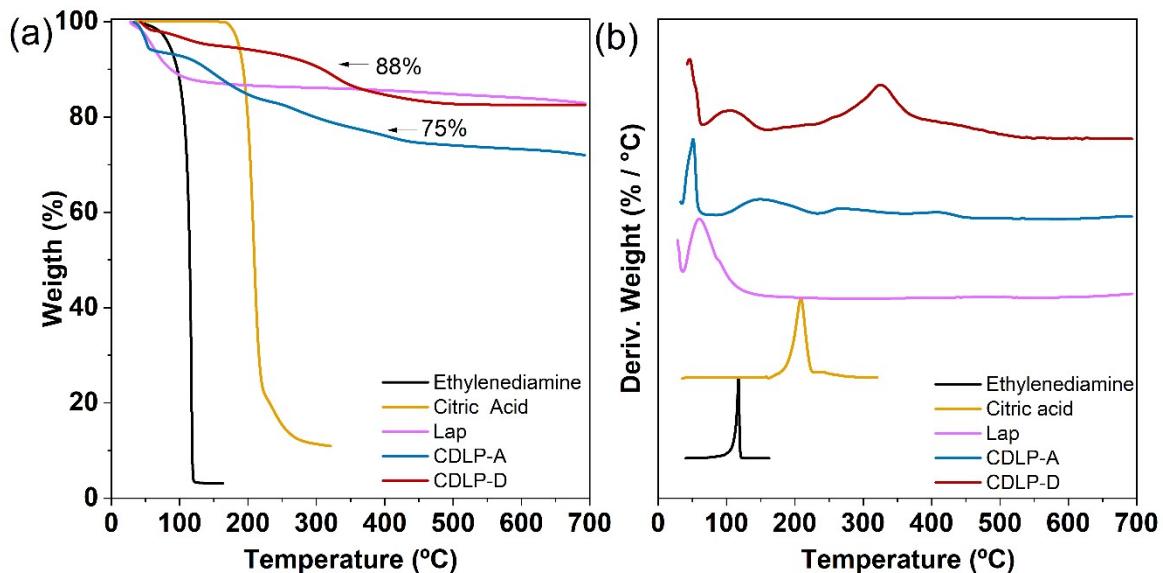

Figure S19. Thermogravimmetic curves (TGA) (a) and derivate termogravimetric curves (DTG) (b). The weight loss was determinated by *TGA curve*, using the event *obtained in DTG* of CDs decomposition, which was 326ºC for CDLP-D and 411 ºC for CDLP-A.

Supplementary Material

Table S3 - CHN elemental analysis for CDLP-A and CDLP-D samples

Samples	% C	% H	% N
CDLP-A	8.0 (±0.2)	2.1 (±0.1)	0.4 (±0.1)
CDLP-D	9.0 (±0.2)	1.6 (±0.1)	2.2 (±0.1)